Estimation Method for Radiation Resistance of Multi-junction Solar Cells using I-V Characteristics of Subcells

Tetsuya Nakamura[1], Mitsuru Imaizumi[1], Mitsunobu Sugai[2], Shin-ichiro Sato[3], and Takeshi Ohshima[3]
1 Japan Aerospace Exploration Agency (JAXA),
2 Advanced Engineering services (AES),
3 Japan Atomic Energy Agency (JAEA),
*Email: nakamura.tetsuya@jaxa.jp
Keyword(s): Photovoltaic cells, Radiation effects, Space technology

Abstract

The radiation degradation characteristic of a multi-junction (MJ) solar cell is more complicated compared to a single-junction (1J) solar cell. To perform the quantitative radiation resistance evaluation of a MJ solar cell, it is necessary to estimate the parameter of subcells in the MJ solar cell, such as the reverse saturation current density (J_0), photo current (I_{photo}) and shunt resistance (R_{sh}). In this work, the technique used to estimate each parameter (J_0, I_{photo}, R_{sh}) of each of the subcells in the MJ solar cell is suggested by combining the electroluminescence (EL) method, which proposed by Fraunhofer group, and the LED bias light (LBL) method. Furthermore, the decline in the maximum power (P_{max}) of the MJ solar cell was predicted on the circuit simulator using this technique before and after 1 MeV electron irradiation.

1. Introduction

Multi-junction (MJ) solar cells of high conversion efficiency are attractive for space use. At present, an InGaP/GaAs/Ge triple-junction (3J) solar cell [1], which efficiently absorbs a broad spectrum of sunlight, is used in space. The inverted metamorphic (IMM) 3J solar cell [2], which is both lightweight and flexible in addition to having high conversion efficiency, attracts considerable attention as a next-generation space solar cell.

To utilize such solar cells in a space environment, we need to experimentally clarify the radiation resistance of their output performance, since this performance declines with exposure to radiation [3]. However, since the MJ solar cell comprises a number of subcells which are electrically connected in series, their degradation behavior is complicated and therefore difficult to understand.

Fig. 1 shows the equivalent circuit of a dual-junction (2J) solar cell, the output current of which is determined with Eq. (1) below.

$$I = I_{photo} - I_{sh} - I_{d1} - I_{d2} \qquad \text{(Eq. 1)}$$

where I_{photo}, I_{sh}, and I_d are the photo, shunt and diode currents, respectively. I_{d1} can be expressed by the diffusion model, and I_{d2} can be expressed by the recombination model. Since I_{sh} and I_d are determined by the shunt resistance (R_{sh}), I_{photo} and the reverse saturation current density (J_0) of all the subcells, it is difficult to estimate I_{sh} and I_d. To evaluate the output current correctly, it turns out that it is necessary to estimate J_0, I_{photo} and R_{sh}.

Recently, it was reported that a new method of estimating the J_0 and open-circuit voltage (V_{oc}) of subcell in a MJ solar cell by using electroluminescence (EL) [4-6] before and after irradiation [7]. In this work, the estimation of each parameter which constitutes an equivalent circuit is enabled by combining the EL method and the LED bias light (LBL) method. In addition, it was adapted before and after 1MeV electron irradiation, and we succeeded in predicting the degradation curve of the maximum power (P_{max}) of the 2J solar cell by obtaining the degradation characteristics of J_0, I_{photo} and R_{sh}.

2. Experimental procedure

We prepared bare type (no coverglass) InGaP/GaAs 2J solar cells which were 2 × 2 cm in size. The cells were irradiated with 1 MeV electrons in fluence up to 1×10^{16} e^-/cm^2 at the Japan Atomic Energy Agency (JAEA). Before and after the irradiation, the current-voltage (IV) characteristics were estimated using EL and LBL methods. The EL method is a technique used to estimate the dark IV (DIV) characteristic of a subcell from the EL emission spectrum [4-7]. Since the MJ solar cell comprises a number of subcells which are connected in series, each subcell DIV characteristic is inseparable in electrical property measurement. However, when the EL method is used, since the emission EL spectra of each subcell differ, the DIV characteristic of each subcell in the MJ solar cell is separable. Conversely, the LBL method is a technique used to estimate the R_{sh} and I_{photo} of each

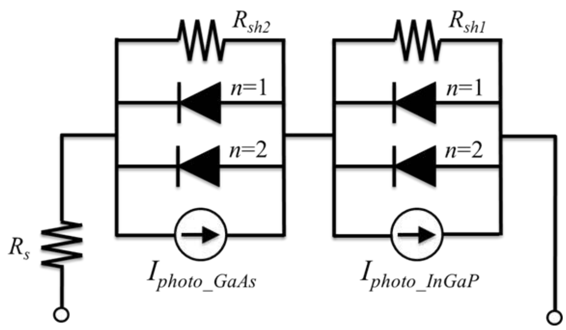

Fig.1: Equation circuit of 2J solar cell

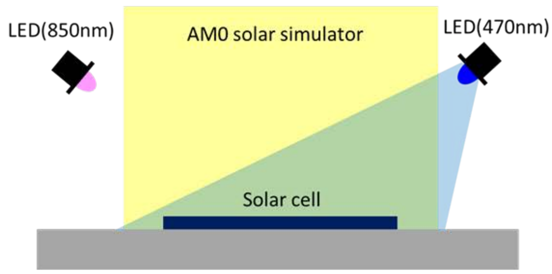

Fig.2: Experimental setup of LBL method

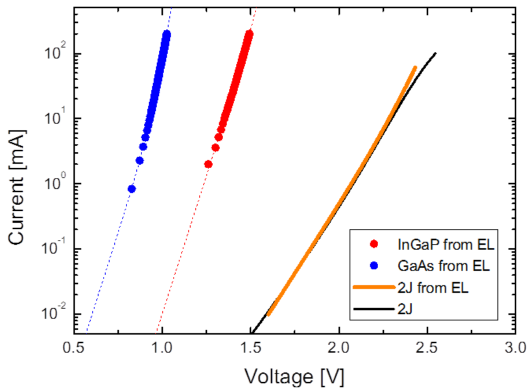

Fig.3: Dark IV characteristics of subcell and 2J solar cell using the EL method before 1MeV electron irradiation.

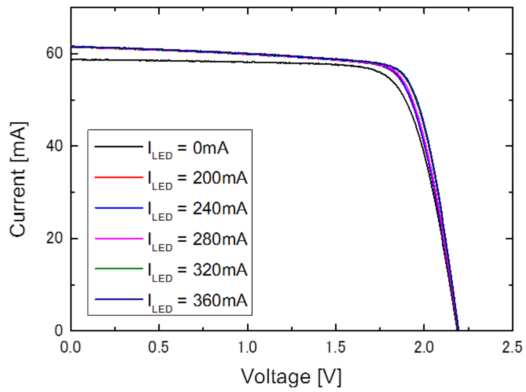

Fig.4: Light IV characteristics of 2J solar cell with 470nm-LED bias light after 1 MeV electron irradiation.

subcell in the MJ solar cell. By irradiating with the solar simulator light adjusted to AM0 and the bias light of LED as shown in Fig. 2, the characteristics of each subcell can be estimated.

3. Results and Discussion

Fig. 3 shows the characteristics of DIV of the 2J solar cell using the EL method before 1 MeV electron irradiation. In Fig. 3, dashed red and blue lines show the DIV characteristics of each subcell, which were fitted by the 2-diode model and obtained with $J_{01\_InGaP} = 6.2 \times 10^{-28}$ A/cm^2, $J_{02\_InGaP} = 9.3 \times 10^{-15}$ A/cm^2, $J_{01\_GaAs} = 1.7 \times 10^{-19}$ A/cm^2, $J_{02\_GaAs} = 2.7 \times 10^{-11}$ A/cm^2, respectively. The merger of the InGaP and GaAs subcell IV, as calculated from the EL method (dashed orange line), correlated well with the actual DIV measurement results (solid black line) of the 2J solar cell, except for series resistance (R_s) and R_{sh}.

Fig. 4 shows the IV curve after 1 MeV electron irradiation. The solid black line is IV curve under the AM0 solar simulator, while the others are under AM0 with a 470nm LED bias light. Since the current-limiting subcell is InGaP subcell under the AM0 solar simulator, R_{sh} of InGaP shows up as an inclination of the plateau region in the solid black line. Conversely, where the injection current into the 470nm LED is 200 mA or more, the short-circuit current (I_{sc}) and inclination of the plateau region are saturated. This inclination shows up R_{sh} of GaAs subcell. If the GaAs subcell is a current-limiting subcell under the AM0 solar simulator, it is irradiated with the 850nm LED, and the current-limit subcell changes to an InGaP subcell.

I_{photo} is calculated by the LBL method and the circuit simulator, SPICE. I_{photo} is also calculated from external quantum efficiency (EQE), but there is no evidence of correlation with the IV curve under AM0 solar simulator. In the case of a MJ solar cell, since there are two or more current generators, measured I_{sc} include I_{photo}, I_d and I_{sh}. Since J_0 and R_{sh} were already estimated, compatibility I_{photo} with the IV curve was calculated by estimating I_d and I_{sh}. The equivalent circuit of Fig. 1 was used in the circuit simulator. Fig. 5 shows I_{sc} of the 2J solar cell and I_{photo}, I_d and I_{sh} of each subcell as a function of 470nm-LED luminescence intensity after 1MeV electron irradiation. Where the luminescence intensity of the LED is zero, the current-limiting subcell was the InGaP subcell. The open black square shows the experimental result of I_{sc} of a 2J solar cell, while others are simulation results. I_{photo} of InGaP and GaAs was calculated by fitting I_{sc} of the experimental results. The red asterisk shows

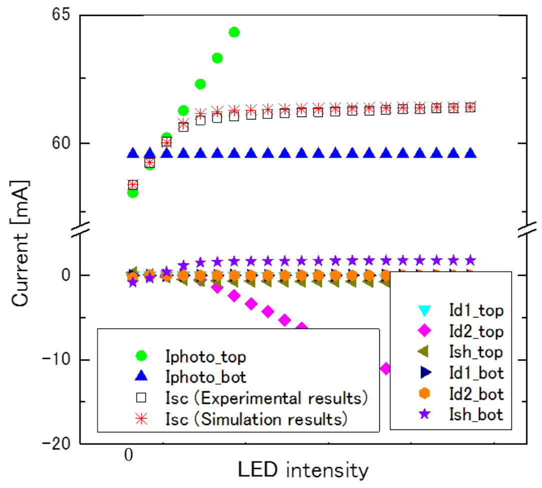

Fig.5: I_{sc} of 2J and the diode and shunt currents of the subcell as a function of 470nm-LED intensity. The open black square shows the experimental results and the other figures are simulation results.

I_{sc} of the circuit simulation results, which correlated well with the open black square. There are two types of change of I_{sc}. In the region where the luminescence intensity of LED is weak, I_{sc} increases to alignment according to the increase in I_{photo} of InGaP (type A). In the region where the luminescence intensity of LED is considerable, I_{sc} is almost unchanged as a function of LED intensity since the current-limiting subcell changes from InGaP to GaAs (type B). In Type A, I_{sc} and I_{photo} of InGaP are almost the same. Conversely, in type B, I_{sc} differs from 2 mA of I_{photo} of GaAs. This is considered to be one factor explaining why the change in R_{sh} in the GaAs subcell with radiation exceeds the InGaP subcell. The advantage of the LBL method is that we can obtain compatibility I_{photo} with an IV curve. The output value obtained by the AM0 solar simulator is compared with the output value of the solar cell, which substitutes each parameter estimated by the LBL and EL methods for the circuit simulator, both of which show good agreement, as shown in the table.

Figure 6 (a) shows the dependence of the remaining factors of I_{photo}, which are obtained by LBL method, on fluence for each subcell after the 1 MeV electron irradiation. The remaining factors of I_{photo} for the InGaP subcell were superior to those of the GaAs subcell. The dashed lines are fitting curves based on the use of Eq. (2) below.

$$I_{photo} = I_{photo\,0} - C_I \log\left(1 + \frac{\Phi}{\Phi_{xI}}\right) \qquad \text{(Eq. 2)}$$

where $I_{photo\,0}$ is initial values before irradiation, C and Φ_x are coefficients computed from the fitting.

The changes in J_{01} and J_{02} for each subcell due to 1 MeV electron irradiation are shown in Fig. 6 (b). Since EL intensity is quite small and cannot be observed in the high fluence region, the estimation result of J_0 is up to 3×10^{15} e^-/cm^2. J_{01} and J_{02} rose with linear increase in fluence. Results which matched and fitted in relative terms were expressed with dotted and solid lines and used to estimate the degradation of P_{max} here in this work.

Figure 6 (c) exhibits the dependence of the reciprocal of R_{sh} on fluence. For lower fluence cases, the R_{sh} of each subcell was sufficiently large hence its change could be ignored. However, a significant decrease of R_{sh} was confirmed in the case of high fluence. Also, with regard to the degradation/decrease of R_{sh}, the InGaP subcell outperformed the GaAs subcell in terms of radiation resistance, which means the radiation resistance of the fill-factor (FF) worsens, when a current-limiting subcell changes from InGaP to the GaAs subcell. Conversely, no degradation/increase of R_s depending upon fluence was distinctly observed or measured.

Based on the results exhibited in Figs. 6 (a) – (c), the degradation trend of P_{max} of the 2J cell was estimated, as indicated with the solid blue line in Fig. 6 (d). J_0, R_{sh} of the current-limiting subcell, and R_{sh} of the 2J cell that determine FF were evaluated using SPICE. The dashed black line shows the fitting result using Eq. (3), which excludes consideration of FF or the current-limiting subcell change for 1J.

$$P_{max} = P_{max_0} - C_P \log\left(1 + \frac{\Phi}{\Phi_{xP}}\right) \qquad \text{(Eq. 3)}$$

There is discrepancy between the dashed and solid lines in the high fluence region, which is attributable to change in the current-limiting subcell from the InGaP to the GaAs subcell at around $\Phi = 3 \times 10^{15}$ e^-/cm^2. Given these findings, this technique is thought to be effective in verifying degradation, especially in the high fluence

Table: Output parameter of the 2J solar cell using the measurement result under the AM0 solar simulator and the circuit simulation results.

	Isc [mA]	Voc [mV]	Pm [mW]	Ipm [mA]	Vpm [mV]
①Solar simulator	58.48	2187	98.06	54.52	1799
②circuit simulator	58.43	2183	98.01	54.88	1786
①/②	100.09%	100.18%	100.05%	99.34%	100.73%

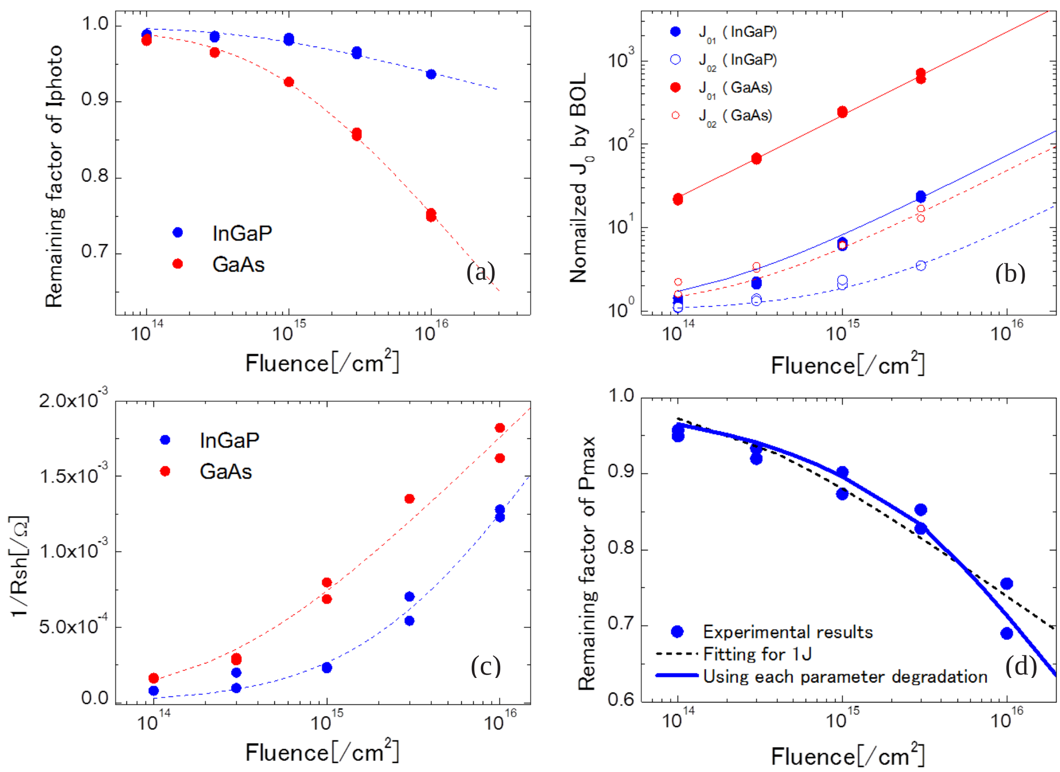

Fig. 5: Characteristics of the radiation resistance of I_{photo}, J_0, R_{sh} and P_{max} in the 2J solar cell after 1MeV electron irradiation. (a) Degradation curves of I_{photo} of the InGaP and GaAs subcells. (b) Degradation curves of J_{01} and J_{02} of the InGaP and GaAs subcells. (c) Degradation curves of $1/R_{sh}$ of the InGaP and GaAs subcells. (d) Degradation curves of P_{max} of the 2J cell. The dashed line was fitted without considering changes in FF and the current-limiting subcell for 1J. The solid line shows the degradation curve with consideration of changes in FF and the current-limiting subcell. The circle indicated experimental results of the remaining factor of P_{max}.

region, which changes a current-limiting subcell. These results promise to allow us to analyze the radiation degradation behavior of MJ cells more precisely, which will help establish a degradation model and consequently an accurate degradation prediction methodology for MJ cells.

4. Summary

The IV characteristics of subcells in InGaP/GaAs 2J solar cells were determined using EL and LBL methods before and after 1 MeV electron irradiation. I_{photo}, J_0 of InGaP and GaAs subcells as well as R_{sh} of each subcell were computed. By obtaining these degradation characteristics, the degradation trend of P_{max} of the 2J solar cell could thus be obtained with sufficient accuracy.

References

[1] M. Yamaguchi et al., "Novel materials for high-efficiency III–V multi-junction solar cells," Sol. Energy, vol. 82, pp.173-180 (2008).
[2] J. F. Geisz et al., "40.8% efficient inverted triple-junction solar cell with two independently metamorphic junctions," Appl. Phys. Lett., vol. 93, 123505 (2008).
[3] D. C. Marvin, "Assessment of Multijunction Solar Cell Performance in Radiation Environments," Aerospace Report, No. TOR-2000(1210)-1 (2000).
[4] U. Rau, "Reciprocity relation between photovoltaic quantum efficiency and electroluminescent emission of solar cells," Phys. Rev. B, vol. 76, 085303 (2007).
[5] T. Kirchartz et al., "Subcell I-V characteristic analysis of GaInP/GaInAs/Ge solar cells using electroluminescence measurements," Appl. Phys. Lett., vol. 92, 123502 (2008).
[6] S. Roensch et al., "Determination of the subcell photovoltage in multijunction solar cells via voltage-dependent capacitance analysis," Appl. Phys. Lett., vol. 98, 251113 (2011).
[7] R. Hoheisel, "Electroluminescence analysis of irradiated GaInP/GaInAs/Ge space solar cells," Sol. Energy Mater. Sol. Cells , in press.